

# Electronic Theory for the Magnetic Anisotropy in $\text{Sr}_2\text{RuO}_4$

I. Eremin,<sup>1,2</sup> D. Manske,<sup>1</sup> J. R. Tarento,<sup>3</sup> and K. H. Bennemann<sup>1</sup>

---

Using a three-band Hubbard Hamiltonian we calculated within the random-phase-approximation the spin susceptibility,  $\chi(\mathbf{q}, \omega)$ , and NMR spin-lattice relaxation rate  $1/T_1$ , in the normal state of the triplet superconductor  $\text{Sr}_2\text{RuO}_4$ , and obtained quantitative agreement with experimental data. Most importantly, we found that because of spin-orbit coupling the out-of-plane component of the spin susceptibility  $\chi^{zz}(\mathbf{q}, \omega)$  becomes two times larger than the in-plane one at low temperatures. We analyze in particular the role of the  $xy$ -band in the magnetic anisotropy.

---

**KEY WORDS:** ruthenates; magnetic dynamics; spin-orbit coupling.

---

The spin-triplet superconductivity with  $T_c = 1.5$  K observed in layered  $\text{Sr}_2\text{RuO}_4$  seems to be a new example of unconventional superconductivity [1]. The non-s-wave symmetry of the order parameter is observed in several experiments (see e.g. Ref. [2,3]). Although the structure of  $\text{Sr}_2\text{RuO}_4$  is the same as for the high- $T_c$  superconductor  $\text{La}_{2-x}\text{Sr}_x\text{CuO}_4$ , its superconducting properties resemble those of superfluid  $\text{He}^3$ . Most recently, it was found that the superconducting order parameter is of p-wave type, but probably contains line nodes between the  $\text{RuO}_2$ -planes [4,5]. These results support Cooper-pairing via spin fluctuations as one of the most probable mechanism to explain the triplet superconductivity in  $\text{Sr}_2\text{RuO}_4$ . Therefore, theoretical and experimental investigations of the spin dynamics behavior in the normal and superconducting state of  $\text{Sr}_2\text{RuO}_4$  are needed.

Here, in addition to our previous study [6], we analyze the normal-state spin dynamics of  $\text{Sr}_2\text{RuO}_4$  by using the two-dimensional three-band Hubbard Hamiltonian and spin-orbit coupling for the all three bands crossing the Fermi level. We calculate the dynamical spin susceptibility  $\chi(\mathbf{q}, \omega)$  within the random-phase-approximation and show that the observed

magnetic anisotropy in the  $\text{RuO}_2$ -plane arises mainly because of the spin-orbit coupling. We demonstrate that as in the superconducting state [7] the spin-orbit coupling plays an important role also for the normal-state spin dynamics of  $\text{Sr}_2\text{RuO}_4$ .

We start from the two-dimensional three-band Hubbard Hamiltonian

$$H = H_t + H_U \sum_{\mathbf{k}, \sigma} \sum_l t_{\mathbf{k}l} a_{\mathbf{k}, l\sigma}^+ a_{\mathbf{k}, l\sigma} + \sum_{i,l} U_l n_{i,l\uparrow} n_{i,l\downarrow}, \quad (1)$$

where  $a_{\mathbf{k}, l\sigma}$  is the Fourier-transformed annihilation operator for the  $d_l$  orbital electrons ( $l = xy, yz, zx$ ) and  $U_l$  is the corresponding on-site Coulomb repulsion.  $t_{\mathbf{k}l}$  denotes the energy dispersions of the tight-binding bands calculated as follows:  $t_{\mathbf{k}l} = -\epsilon_0 - 2t_x \cos k_x - 2t_y \cos k_y + 4t' \cos k_x \cos k_y$ . We choose the values for the parameter set  $(\epsilon_0, t_x, t_y, t')$  as (0.5, 0.42, 0.44, 0.14), (0.24, 0.31, 0.045, 0.01), and (0.24, 0.045, 0.35, 0.01) eV for  $d_{xy^-}$ ,  $d_{zx^-}$ , and  $d_{yz^-}$  orbitals in accordance with band-structure calculations [8]. The electronic properties of this model in application to  $\text{Sr}_2\text{RuO}_4$  were studied recently and as was found can explain some features of the spin excitation spectrum in  $\text{Sr}_2\text{RuO}_4$  [9,7,10,11]. However, this model fails to explain the observed magnetic anisotropy at low temperatures [12]. On the other hand, it is known that spin-orbit coupling plays an important role in the superconducting state of  $\text{Sr}_2\text{RuO}_4$  [7]. This is further confirmed by the recent observation of large

<sup>1</sup>Institut für Theoretische Physik, Freie Universität Berlin, D-14195 Berlin, Germany.

<sup>2</sup>Physics Department, Kazan State University, 420008 Kazan, Russia.

<sup>3</sup>Laboratoire de Physique des Solides, Université d'Orsay, Batiment 510, 91400 Orsay, France.

spin-orbit coupling in insulating  $\text{Ca}_2\text{RuO}_4$  [13]. Therefore, we include spin-orbit coupling in our model:

$$H_{\text{so}} = \lambda \sum_i L_i S_i, \quad (2)$$

where the angular momentum  $L_i$  operates on the three  $t_{2g}$ -orbitals on the site  $i$ . Similar to an earlier approach [7], we restrict ourselves to the three orbitals, ignoring  $e_{2g}$ -orbitals and choose the coupling constant  $\lambda$  such that the  $t_{2g}$ -states behave like an  $l = 1$  angular momentum representation. The resulting  $6 \times 6$  matrix has the form:

$$H_t + H_{\text{so}} = \begin{pmatrix} t_{\mathbf{k},xy} & 0 & 0 & -\frac{\lambda}{2} & 0 & i\frac{\lambda}{2} \\ 0 & t_{\mathbf{k},xy} & \frac{\lambda}{2} & 0 & i\frac{\lambda}{2} & 0 \\ 0 & \frac{\lambda}{2} & t_{\mathbf{k},yz} & 0 & -i\frac{\lambda}{2} & 0 \\ -\frac{\lambda}{2} & 0 & 0 & t_{\mathbf{k},yz} & 0 & i\frac{\lambda}{2} \\ 0 & -i\frac{\lambda}{2} & i\frac{\lambda}{2} & 0 & t_{\mathbf{k},xz} & 0 \\ -i\frac{\lambda}{2} & 0 & 0 & -i\frac{\lambda}{2} & 0 & t_{\mathbf{k},xz} \end{pmatrix}.$$

One notices that the degeneracy with respect to a spin projection is not removed by the spin-orbit coupling (so-called Kramers degeneracy). Therefore, the  $6 \times 6$  matrix decouples into two matrices  $3 \times 3$ . Furthermore, it is known that the quasi-two-dimensional  $xy$ -band is separated from the quasi-one-dimensional  $xz$ - and  $yz$ -bands. Then, one expects that the effect of spin-orbit coupling is small for  $xy$ -band and can be included in the approximate way. In particular, we suggest that the dispersion of the  $xy$ -band will be unchanged and  $\epsilon_{\mathbf{k},xy}^\sigma \approx t_{\mathbf{k},xy}$ . Then, other eigenvalues of the matrix can be found and the new energy dispersions are

$$\epsilon_{\mathbf{k},yz}^\sigma \approx (t_{\mathbf{k},yz} + t_{\mathbf{k},xz} + A_{\mathbf{k}})/2, \quad (3)$$

$$\epsilon_{\mathbf{k},xz}^\sigma \approx (t_{\mathbf{k},yz} + t_{\mathbf{k},xz} + A_{\mathbf{k}})/2,$$

where  $A_{\mathbf{k}} = \sqrt{(t_{\mathbf{k},yz} - t_{\mathbf{k},xz})^2 + 3\lambda^2}$ , and  $\sigma$  refers to spin projection.

The resultant Fermi surface consists of three sheets like observed in the experiment. Most importantly, spin-orbit coupling together with Eq. (1) leads to a new quasiparticle which we label by pseudo-spin and pseudo-orbital indices. The unitary transformation  $\tilde{U}_{\mathbf{k}}$  connecting old and new quasiparticles is defined for each wave vector and lead to the following relation between them

$$\begin{aligned} c_{\mathbf{k},yz+}^+ &= u_{1\mathbf{k}} a_{\mathbf{k},yz+}^+ - i v_{1\mathbf{k}} a_{\mathbf{k},xz+}^+ + v_{1\mathbf{k}} a_{\mathbf{k},xy-}^+, \\ c_{\mathbf{k},xz+}^+ &= u_{2\mathbf{k}} a_{\mathbf{k},yz+}^+ - i v_{2\mathbf{k}} a_{\mathbf{k},xz+}^+ + v_{2\mathbf{k}} a_{\mathbf{k},xy-}^+, \end{aligned}$$

$$\begin{aligned} c_{\mathbf{k},xy-}^+ &= u_{3\mathbf{k}} a_{\mathbf{k},yz+}^+ - i v_{3\mathbf{k}} a_{\mathbf{k},xz+}^+ + v_{3\mathbf{k}} a_{\mathbf{k},xy-}^+, \\ c_{\mathbf{k},yz+} &= -u_{1\mathbf{k}} a_{\mathbf{k},yz+}^+ - i v_{1\mathbf{k}} a_{\mathbf{k},xz+}^+ + v_{1\mathbf{k}} a_{\mathbf{k},xy-}^+, \\ c_{\mathbf{k},xz+} &= -u_{2\mathbf{k}} a_{\mathbf{k},yz+}^+ - i v_{2\mathbf{k}} a_{\mathbf{k},xz+}^+ + v_{2\mathbf{k}} a_{\mathbf{k},xy-}^+, \\ c_{\mathbf{k},xy-} &= -u_{3\mathbf{k}} a_{\mathbf{k},yz+}^+ - i v_{3\mathbf{k}} a_{\mathbf{k},xz+}^+ + v_{3\mathbf{k}} a_{\mathbf{k},xy-}^+, \end{aligned} \quad (4)$$

where

$$\begin{aligned} u_{m\mathbf{k}} &= \frac{t_{\mathbf{k},xz} - t_{\mathbf{k},yz} \mp A_{\mathbf{k}} - \lambda}{\sqrt{2(t_{\mathbf{k},xz} - t_{\mathbf{k},yz})^2 + 2(\lambda \pm A_{\mathbf{k}})^2 + \lambda^2}}, \\ v_{m\mathbf{k}} &= \frac{t_{\mathbf{k},yz} - t_{\mathbf{k},xz} \mp A_{\mathbf{k}} - \lambda}{\sqrt{2(t_{\mathbf{k},xz} - t_{\mathbf{k},yz})^2 + 2(\lambda \pm A_{\mathbf{k}})^2 + \lambda^2}}, \\ v_{m\mathbf{k}} &= \frac{2\lambda}{\sqrt{2(t_{\mathbf{k},xz} - t_{\mathbf{k},yz})^2 + 2(\lambda \pm A_{\mathbf{k}})^2 + \lambda^2}}. \end{aligned}$$

The “-” and “+” signs refer to the  $m = 1$  and  $m = 2$ , respectively. In the similar way, one obtains

$$\begin{aligned} u_{3\mathbf{k}} &= \frac{(t_{\mathbf{k},xz} - t_{\mathbf{k},xy}) \left(\frac{\lambda}{2}\right) - \frac{\lambda^2}{4}}{N}, \\ v_{3\mathbf{k}} &= \frac{(t_{\mathbf{k},yz} - t_{\mathbf{k},xy}) \left(\frac{\lambda}{2}\right) - \frac{\lambda^2}{4}}{N}, \\ v_{3\mathbf{k}} &= \frac{\text{sign}((t_{\mathbf{k},xz} - t_{\mathbf{k},xy})(t_{\mathbf{k},yz} - t_{\mathbf{k},xy}) - \frac{\lambda^2}{4})}{N}, \end{aligned}$$

where  $N$  is determined from the normalization of the eigenvector. One could also see that different new eigenstates are only approximately orthogonal to each other. This is due to approximations which we have made for finding the eigenvalues. However, one estimates that the error of the order of  $O(\lambda^2)$  that indicates the equivalence of our procedure to an effective second order perturbation theory.

For the calculation of the transverse,  $\chi_l^{+-}$ , and longitudinal,  $\chi_l^{zz}$ , components of the spin susceptibility of each band  $l$  we use the diagrammatic representation. Since the Kramers degeneracy is not removed by the spin-orbit coupling, the main anisotropy arises from the calculations of the anisotropic vertex  $g_z = \tilde{l}_z + 2s_z$  and  $g_+ = \tilde{l}_+ + 2s_+$  calculated on the basis of the new quasiparticle states. In addition, because of the hybridization between  $xz$ - and  $yz$ -bands we also calculate the transverse and longitudinal components of the the interband susceptibility  $\chi_w$ . Then, for example,

$$\begin{aligned} \chi_{0,xz}^{+-}(\mathbf{q}, \omega) &= -\frac{1}{N} \sum_{\mathbf{k}} |M_{\mathbf{k},\mathbf{k}+\mathbf{q}}^{+-}|^2 \\ &\times \frac{f(\epsilon_{\mathbf{k}xz}^+) - f(\epsilon_{\mathbf{k}+\mathbf{q}xz}^-)}{\epsilon_{\mathbf{k}xz}^+ - \epsilon_{\mathbf{k}+\mathbf{q}xz}^- + \omega + iO^+}, \end{aligned} \quad (5)$$

and

$$\chi_{0,yz}^{zz}(\mathbf{q}, \omega) = -\frac{1}{N} \sum_{\mathbf{k}} |M_{\mathbf{k},\mathbf{k}+\mathbf{q}}^{zz}|^2 \times \frac{f(\epsilon_{\mathbf{k}xz}^+) - f(\epsilon_{\mathbf{k}+\mathbf{q}xz}^+)}{\epsilon_{\mathbf{k}xz}^+ - \epsilon_{\mathbf{k}+\mathbf{q}xz}^- + \omega + i0^+}, \quad (6)$$

where  $f(x)$  is the Fermi function and  $|M_{\mathbf{k},\mathbf{k}+\mathbf{q}}^i|^2 = |\langle l|g_i|l' \rangle|^2$  are the corresponding matrix elements calculated with the help of Eqs. (4). For all other orbitals the calculations are straightforward.

Assuming  $U_{ij} = \sigma_{ij}U$  one gets the following expressions for the transverse susceptibility within random-phase-approximation (RPA):

$$\chi_{RPA,i}^{+-}(\mathbf{q}, \omega) = \frac{\chi_{0,i}^{+-}(\mathbf{q}, \omega)}{1 - U\chi_{0,i}^{+-}(\mathbf{q}, \omega)}, \quad (7)$$

and for the longitudinal susceptibility

$$\chi_{RPA,i}^{zz}(\mathbf{q}, \omega) = \frac{\chi_{0,i}^{\uparrow}(\mathbf{q}, \omega) + \chi_{0,i}^{\downarrow}(\mathbf{q}, \omega) + 2U\chi_{0,i}^{\uparrow}(\mathbf{q}, \omega)\chi_{0,i}^{\downarrow}(\mathbf{q}, \omega)}{1 - U^2\chi_{0,i}^{\downarrow}(\mathbf{q}, \omega)\chi_{0,i}^{\uparrow}(\mathbf{q}, \omega)}. \quad (8)$$

Figure 1 shows the results for the real part of the transverse and longitudinal total susceptibility,  $\chi_{RPA}^{+-,zz} = \sum_i \chi_{RPA,i}^{+-,zz}$  along the route  $(0, 0) \rightarrow (\pi, 0) \rightarrow (\pi, \pi) \rightarrow (0, 0)$  in the first Brillouin zone for  $U = 0.505$  eV. Note the important difference between the two components. Most importantly, the incommensurate antiferromagnetic fluctuations (IAF) at

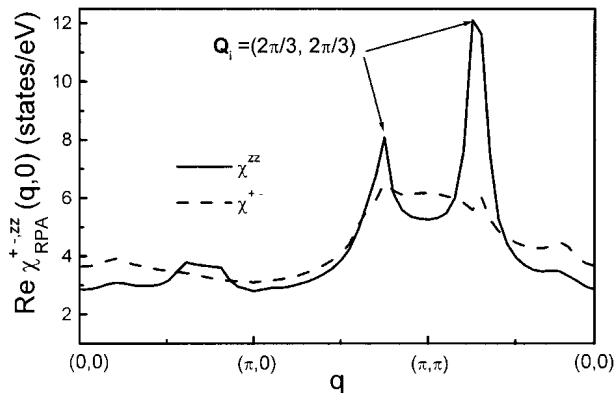


**Fig. 1.** Results for the real part of out-of-plane (solid curve) and in-plane (dashed curve) magnetic susceptibilities,  $\text{Re } \chi(\mathbf{q}, \omega)$ , calculated within RPA by using  $U = 0.505$  eV along the two-dimensional route  $(0, 0) \rightarrow (\pi, 0) \rightarrow (\pi, \pi) \rightarrow (0, 0)$  within the first Brillouin zone at temperature  $T = 100$  K.

$\mathbf{Q}_i = (2\pi/3, 2\pi/3)$  are present in the case of  $xz$ - and  $yz$ -bands *only* in the longitudinal components of the spin susceptibility, but not in the transverse ones. This is connected to the fact that the matrix elements type of  $u_{\mathbf{k}}$  and  $v_{\mathbf{k}}$  are important because they suppress transition between “+” and “-” bands for the transverse susceptibilities. The transverse susceptibility is larger than the longitudinal one at small values of  $\mathbf{q}$  indicating ferromagnetic fluctuations. These are mainly pointing in the RuO<sub>2</sub>-plane. On the other hand, the longitudinal component shows a structure at the IAF wave vector indicating a direction of the IAF fluctuations perpendicular to the RuO<sub>2</sub>-plane. Our results are similar our previous studies [6] where the effect of spin-orbit coupling for  $xy$ -band was excluded, for simplicity. This also indicates that the magnetic properties of the  $\gamma$ -band remains almost unaffected by the spin-orbit coupling.

We also note that our results are in accordance with earlier estimations made by Ng and Sigrist [14] with one important difference. In addition to Ng and Sigrist [14], we include in accordance with mixing of the spin and orbital degrees of freedom also the orbital contribution to the magnetic susceptibility  $\chi$ . For example, because of  $l_z$  and  $l_{\pm}$  ( $l_{-}$ ) vertices at  $\mathbf{Q}_i = (2\pi/3, 2\pi/3)$ ,  $\chi^{zz}$  is affected by factor of 2 from spin-orbit coupling. Moreover, in previous work [14], it was found that the IAF are slightly enhanced in the longitudinal components of the  $xz$ - and  $yz$ -bands in comparison to the transverse one. In our case there are *no* IAF in the transverse component of the spin susceptibility. Furthermore, by taking into account the correlation effects within RPA we show that the IAF will be further enhanced in the  $z$ -direction.

Finally, in order to compare our results with experimental data we calculate the nuclear spin-lattice relaxation rate for <sup>17</sup>O ion in the RuO<sub>2</sub>-plane for different external magnetic field orientation ( $i = a, b,$  and  $c$ )

$$\left[ \frac{1}{T_1 T} \right]_i = \frac{2k_B \gamma_n^2}{(\gamma_e \hbar)^2} \sum_{\mathbf{q}} |A_{\mathbf{q}}^p|^2 \frac{\chi_p''(\mathbf{q}, \omega_{sf})}{\omega_{sf}}, \quad (9)$$

where  $A_{\mathbf{q}}^p$  is the  $q$ -dependent hyperfine-coupling constant and  $\chi_p''$  is the imaginary part of the corresponding spin susceptibility, respectively, *perpendicular* to the  $i$ -direction. Similar to experiment [12] we use an isotropic hyperfine coupling constant ( $^{17}A_{\mathbf{q}} \sim 22$  kOe/ $\mu_B$ ).

Figure 2 shows the calculated temperature dependence of the spin-lattice relaxation for an external magnetic field within and perpendicular to

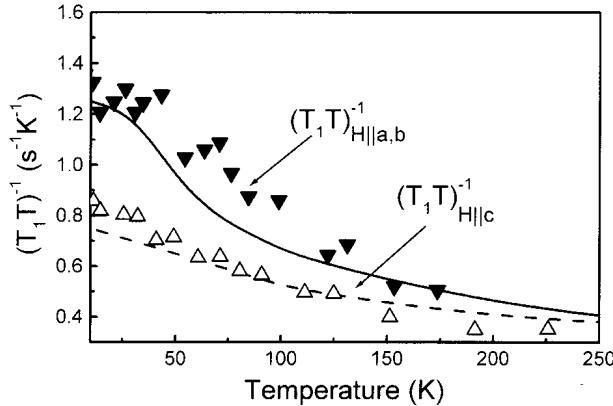


**Fig. 2.** Calculated normal state temperature dependence of the nuclear spin-lattice relaxation rate  $T_1^{-1}$  of  $^{17}\text{O}$  in the  $\text{RuO}_2$ -plane for the external magnetic field applied along  $c$ -axis (dashed curve) and along the  $ab$ -plane (solid curve). Down- and up-triangles are experimental points taken from Ref. [12] for the corresponding magnetic field direction.

the  $\text{RuO}_2$ -plane together with experimental data. At  $T = 250$  K the spin-lattice relaxation rate is almost isotropic. Because of the anisotropy in the spin susceptibilities arising from spin-orbit coupling the relaxation rates become different with decreasing temperature. The largest anisotropy occurs close to the superconducting transition temperature in good agreement with experimental data [12].

To summarize, our results clearly demonstrate the essential significance of spin-orbit coupling for the spin-dynamics already in the normal state of the triplet superconductor  $\text{Sr}_2\text{RuO}_4$ . We find that the magnetic response becomes strongly anisotropic even within a  $\text{RuO}_2$ -plane: while the in-plane response is mainly ferromagnetic, the out-of-plane response is antiferromagnetic-like. We would like to stress that our calculations are purely two-dimensional and the discussion of magnetic anisotropy refers only to the

$\text{RuO}_2$ -plane. It remains, however, to see how the two-dimensional properties of  $\text{Sr}_2\text{RuO}_4$  can be affected by the magnetic anisotropy. One could expect, for example, the significant interplane magnetic activity induced by some kind of RKKY interaction resulting from the anisotropic  $\chi_{zz}$ .

## ACKNOWLEDGMENTS

We are grateful to INTAS (Grant No. 01-654) and German-French Foundation (PRO-COPE) for the financial support. The work of I. Eremin is supported by the Alexander von Humboldt Foundation and CRDF (Grant No. REC. 007).

## REFERENCES

1. Y. Maeno, H. Hashimoto, K. Yoshida, S. Nishizaki, T. Fujita, J. G. Bednorz, and F. Lichtenberg, *Nature* **372**, 532 (1994).
2. K. Ishida, Y. Kitaoka, K. Asayama, S. Ikeda, S. Nishizaki, Y. Maeno, K. Yoshida, and T. Fujita, *Phys. Rev. B* **56**, R505 (1997).
3. J. A. Duffy, S. M. Hayden, Y. Maeno, Z. Mao, J. Kulda, and G. J. McIntyre, *Phys. Rev. Lett.* **85**, 5412 (2000).
4. M. A. Tanatar, M. Suzuki, S. Nagai, Z. Q. Mao, Y. Maeno, and T. Ishiguro, *Phys. Rev. Lett.* **86**, 2649 (2001).
5. K. Izawa, H. Takahashi, H. Yamaguchi, Y. Matsuda, M. Suzuki, T. Sasaki, T. Fukase, Y. Yoshida, R. Settai, and Y. Onuki, *Phys. Rev. Lett.* **86**, 2649 (2001).
6. I. Eremin, D. Manske, and K. H. Bennemann, *Phys. Rev. B* **65**, R220502 (2002).
7. K. K. Ng and M. Sigrist, *Europhys. Lett.* **49**, 473 (2000).
8. A. Liebsch and A. Lichtenstein, *Phys. Rev. Lett.* **84**, 1591 (2000).
9. I. I. Mazin and D. J. Singh, *Phys. Rev. Lett.* **82**, 4324 (1999).
10. D. K. Morr, P. F. Trautman, and M. J. Graf, *Phys. Rev. Lett.* **86**, 5978 (2001).
11. I. Eremin, D. Manske, C. Joas, and K. H. Bennemann, *Europhys. Lett.* **58**, 871 (2002).
12. K. Ishida, H. Mukuda, Y. Minami, Y. Kitaoka, Z. Q. Mao, H. Fukazawa, and Y. Maeno, *Phys. Rev. B* **64**, 100501(R) (2001).
13. T. Mizokawa, L. H. Tjeng, G. A. Sawatzky, G. Ghiringhelli, O. Tjernberg, N. B. Brookes, H. Fukazawa, S. Nakatsuji, and Y. Maeno, *Phys. Rev. Lett.* **87**, 077202 (2001).
14. K. K. Ng and M. Sigrist, *J. Phys. Soc. Jpn.* **69**, 3764 (2000).